UNCLASSIFIED

SECURITY CLASSIFICATION OF THIS PAGE

FILE COPY

(2)

REPORT DOCUMENTATION PAGE

EPORT SECURITY CLASSIFICATION UNCLASSIFIED	1b. RESTRICTIVE MARKINGS
2a. SECURITY CLASSIFICATION **AD-A217 199** S)	3. DISTRIBUTION/AVAILABILITY OF REPORT Approved for public release; distribution unlimited.
	5. MONITORING ORGANIZATION REPORT NUMBER(S) AFOSR-TR- 89-1852
6a. NAME OF PERFORMING ORGANIZATION CARNEGIE-MELLON UNIVERSITY 6b. OFFICE SYMBOL (If applicable)	7a. NAME OF MONITORING ORGANIZATION AIR FORCE OFFICE OF SCIENTIFIC RESEARCH
6c. ADDRESS (City, State and ZIP Code) PITTSBURGH, PA 15213	7b. ADDRESS (City, State and ZIP Code) BOLLING AFB DC 20332-6448
8a. NAME OF FUNDING/SPONSORING ORGANIZATION AIR FORCE OFFICE OF SCIENTIFIC RESEARCH 8b. OFFICE SYMBOL (If applicable) NA	9. PROCUREMENT INSTRUMENT IDENTIFICATION NUMBER AFOSR 80-0203
8c. ADDRESS (City, State and ZIP Code) BOLLING AFB DC 20332-6448	10. SOURCE OF FUNDING NOS. PROGRAM ELEMENT NO. 61102F; PROJECT NO. 2308; TASK NO. A2; WORK UNIT NO.
11. TITLE (Include Security Classification) MULTIPLE IGNITION, COMBUSTION AND QUENCHING OF HYDROCARBON FUEL SPRAYS	

PERSONAL AUTHOR(S)
AGGARWAL; R BISHOP; W A SIRIGNANO; H T SOMMER

13a. TYPE OF REPORT	13b. TIME COVERED	14. DATE OF REPORT (Yr., Mo., Day)	15. PAGE COUNT
ANNUAL	FROM 01JUL81 TO 30 JUN 82	1982, DECEMBER	40

16. SUPPLEMENTARY NOTATION

17. COSATI CODES			18. SUBJECT TERMS (Continue on reverse if necessary and identify by block number)
FIELD	GROUP	SUB. GR.	

19. ABSTRACT (Continue on reverse if necessary and identify by block number)

DISTRIBUTION/AVAILABILITY OF ABSTRACT CLASSIFIED/UNLIMITED ☐ SAME AS RPT. ☐ DTIC USERS ☐	21. ABSTRACT SECURITY CLASSIFICATION Uncl
22a. NAME OF RESPONSIBLE INDIVIDUAL JULIAN M TISHKOFF	22b. TELEPHONE NUMBER (Include Area Code) (202) 767-4935 22c. OFFICE SYMBOL AFOSR/NA

DD FORM 1473, 83 APR EDITION OF 1 JAN 73 IS OBSOLETE.

UNCLASSIFIED

SECURITY CLASSIFICATION OF THIS PAGE

ABSTRACT

Ignition data has been compiled for combustible gaseous mixtures with hot burning particle sources. High-speed photography, Schlieren photography, pyrometry have been employed in the diagnostics. The ignition and non-ignition domains in terms of particle size and mixture ratio have been determined. The design and fabrication of the spray ignition experiment is underway. Finite-difference and asymptotic results have been obtained for the analysis of gaseous mixture ignition. These analyses have been concluded and the ignition domains have been determined with good agreement (within our limitations of knowledge about chemical kinetics) have been obtained. The preliminary theoretical results about spray ignition indicated that minimum ignition energy and ignition delay should be treated as probabilistic parameters.

OBJECTIVES

The direction of this study has been a continuation of compiling ignition data of combustible mixtures ignited by burning particles. Additionally, different materials have been used to ignite the fuel/air mixtures to help in the understanding of the processes involved in ignition.

Further, the technical objective has been to gain a fundamental scientific understanding of the phenomenon of multiple ignition. Emphasis was placed on the process leading to flame establishment in practical situations. Both homogeneous and heterogeneous combustible hydrocarbon/air mixtures were considered. Also, two kinds of ignition sources were considered:

i. inert, and

ii. burning sources (i.e., burning metals).

Individual ignition sources of sub-millimeter scale and their local combustible environment were examined in a way that both structure and global behavior were resolved. The theoretical approach involves finite-difference calculations to resolve spatially and temporally the behavior of temperature and concentration in the vicinity of the ignition source due to the combined processes of heat and mass transfer, chemical reaction, fuel droplet heating and vaporization, and expanding gases.

ACHIEVEMENTS

INTRODUCTORY COMMENTS

There have been very limited spray ignition studies, experimental or theoretical, which are reported in the literature. Miyasaka and Mizutani [5,6] used shock tube techniques to study the ignition of a premixed spray column. From their experimental results, they obtained correlations which indicate a strong influence of temperature, oxygen concentration, drop size, fuel type, and a weak influence of pressure on the ignition delay time. Ballal and Lefebvre [7,8] have reported experimental as well as analytical results for the spark ignition of homogeneous and heterogeneous fuel-air mixtures. They obtained extensive experimental results which give the effects of various physical and chemical parameters on the quenching distance and the minimum ignition energy. Their analytical results, however, were based on a very simplified model, whereby the time required for the fuel evaporation and burning was compared with the time required for a hot spherical kernel (created by the spark) to get quenched by losing heating to its surroundings. A similar

approach was followed by Peters and Mellor [9] to develop an ignition model for quiescent fuel spray. They compared the time of heat removal from the spark kernel to the fuel evaporation time. Their results also show favorable comparison with the experimental data of Ballal and Lefebvre [7]. Chan and Polymeropoulos [10] used electric sparks for the ignition of laminar tetralin-air monodisperse sprays, where they varied the droplet diameter from 8 to 32 μm. Their results indicate that the ignition energy first decreases as the drop size is decreased, and then start increasing with a further decrease in the drop size.

EXPERIMENTAL PROGRAM

Experiments with burning magnesium particles in methane/air mixtures have been conducted to identify the effect of different metals on the ignition limit. It has been experimentally found that magnesium particles can safely burn in a methane/air mixture despite the fact that their size corresponds to a burning energy significantly greater than that which is able to ignite the mixture by a burning aluminum particle. This data is presented in Figure 1. As this cannot be explained by their difference in energy of combustion, it is speculated that other processes such as catalysis or radiation might be involved.

During the last funding period and the first few months of the current funding period, existing diagnostic techniques have been improved and complemented. The existing diagnostic techniques can be separated into two types:

- optical methods to observe and record the short time ignition and particle burning process, and
- methods to characterize the initial and environmental conditions of the test gas and the particle.

Four optical signals are used to analyze the ignition of combustible mixtures by burning metal particles. A sensitive photon detector records the photon current from the combustion bomb generated by the laser pulse, the burning particle, or the combustion of the gas mixture. Oscilloscope traces of the photo multiplier are used to identify the different stages of the ignition process. During the first half of the current funding period, measures have been taken to improve the photo multiplier signal quality and resolution. These steps resulted in more detailed information about the particle ignition and burning process itself, and the time delay between particle burnout and gas ignition.

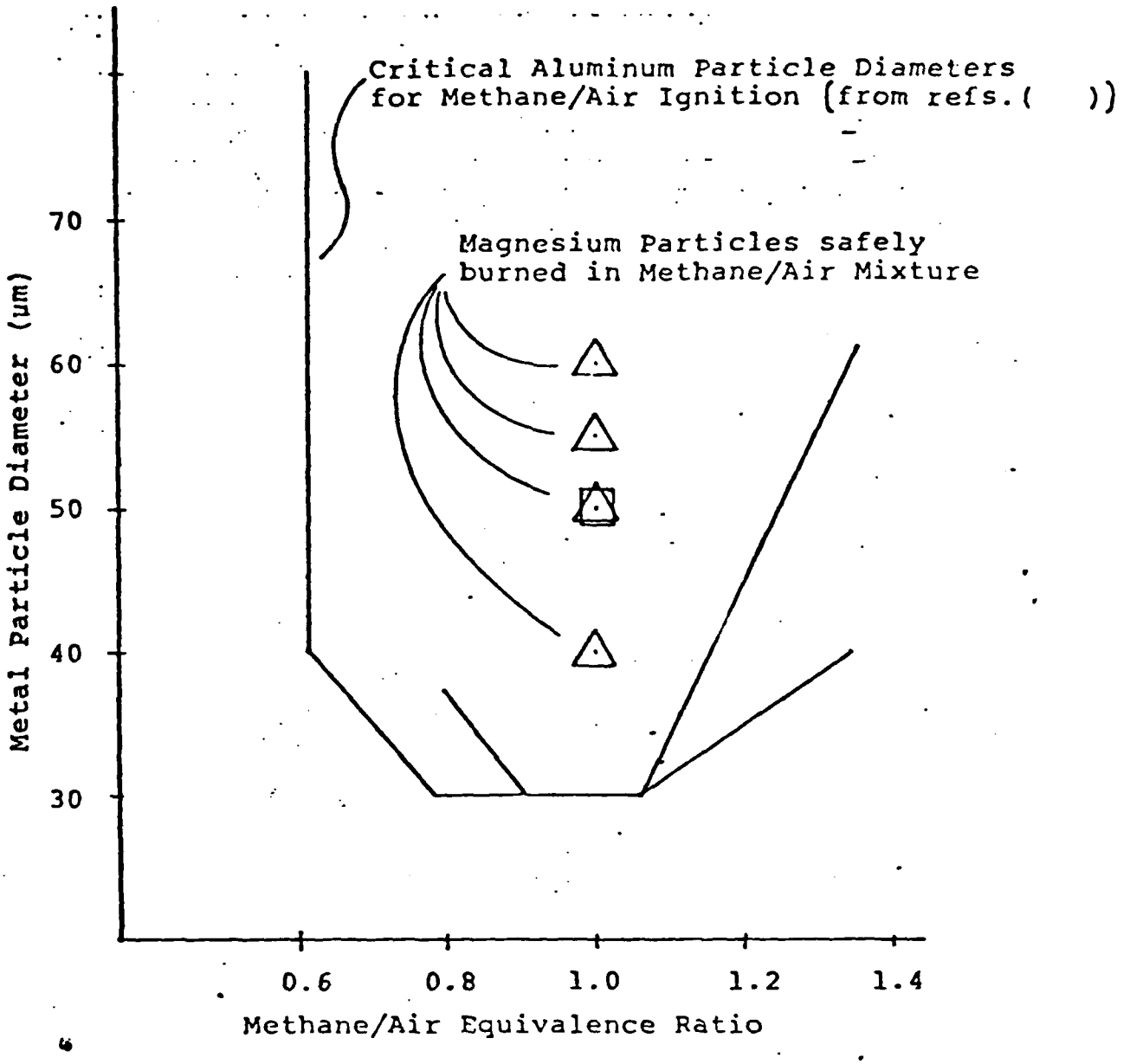

Figure 1: Burning Aluminum and Magnesium Particle Ignition of Methane

A high-speed (up to 10,000 frames/second) movie camera was installed to record the history of the burning particle and to resolve the rapid ignition event. The laser beam was triggered by the camera when the film was accelerated up to the selected number of frames per second. The camera was focused on the particle through windows in the test section. A large magnification of the particle area is necessary to collect enough light emitted from the particle onto the film. The analysis of several films show that the burning particle is moving. An explanation for this motion might be a jet effect due to metal oxide being accelerated away from the particle when it is ignited locally on the surface. Unfortunately, the intensity of the

light emitted during the burning of the particle is too low to allow it to cover a larger viewing area. In the future, Schlieren photography will help to overcome this disadvantage.

The installation of a three-color pyrometer was completed during the last few months. This new diagnostic technique will enable us to measure the surface temperature of the burning particle. The temperature information will help to identify the influence of the particle surface temperature igniting the fuel-air mixture.

The experimental technique to determine the toluene-air mixture ratio was changed and improved. In reviewing the procedure to fill the combustion vessel with a known toluene-air mixture, an error source was detected which was not considered during the earlier experiments. It was observed that condensation occurred in the lines feeding the toluene saturated air into the combustion chamber. The former experimental procedure assumed that the combustion vessel was supplied with toluene saturated air and the required toluene/air equivalence ratio was established by adding pure air. Since condensation decreased the amount of toluene in the combustion bomb, the actual equivalence ratio was lower than the one based on the assumption to mix toluene-saturated air. It is not possible with the existing experimental apparatus to establish a toluene-vapor-air mixture of known ratio by balancing the mass flow of toluene/air to the bomb. The direct measurement of the toluene-vapor content by means of a gas chromatography was established as a routine procedure. Careful calibration of the gas chromotograph and elimination of possible error sources during the probe extraction improved the reproducibility and accuracy of the measured equivalence ratio. Figure 2 gives data for particle sizes igniting or burning without igniting different toluene vapor air mixtures. These data compared to data taken during former experiments appear at lower equivalence ratios. The data differs from that reported by Stanley [1], although a greater degree of confidence exists for the results presented herein.

The design and construction of the experimental system to test ignition of sprays with large droplets (10-100 μm) is underway. The problems associated with condensation of toluene in the feeding lines of the system appear here too, resulting in a stratification effect in the test section.

THEORETICAL PROGRAM

The theoretical development of the ignition of combustible gaseous mixtures by hot

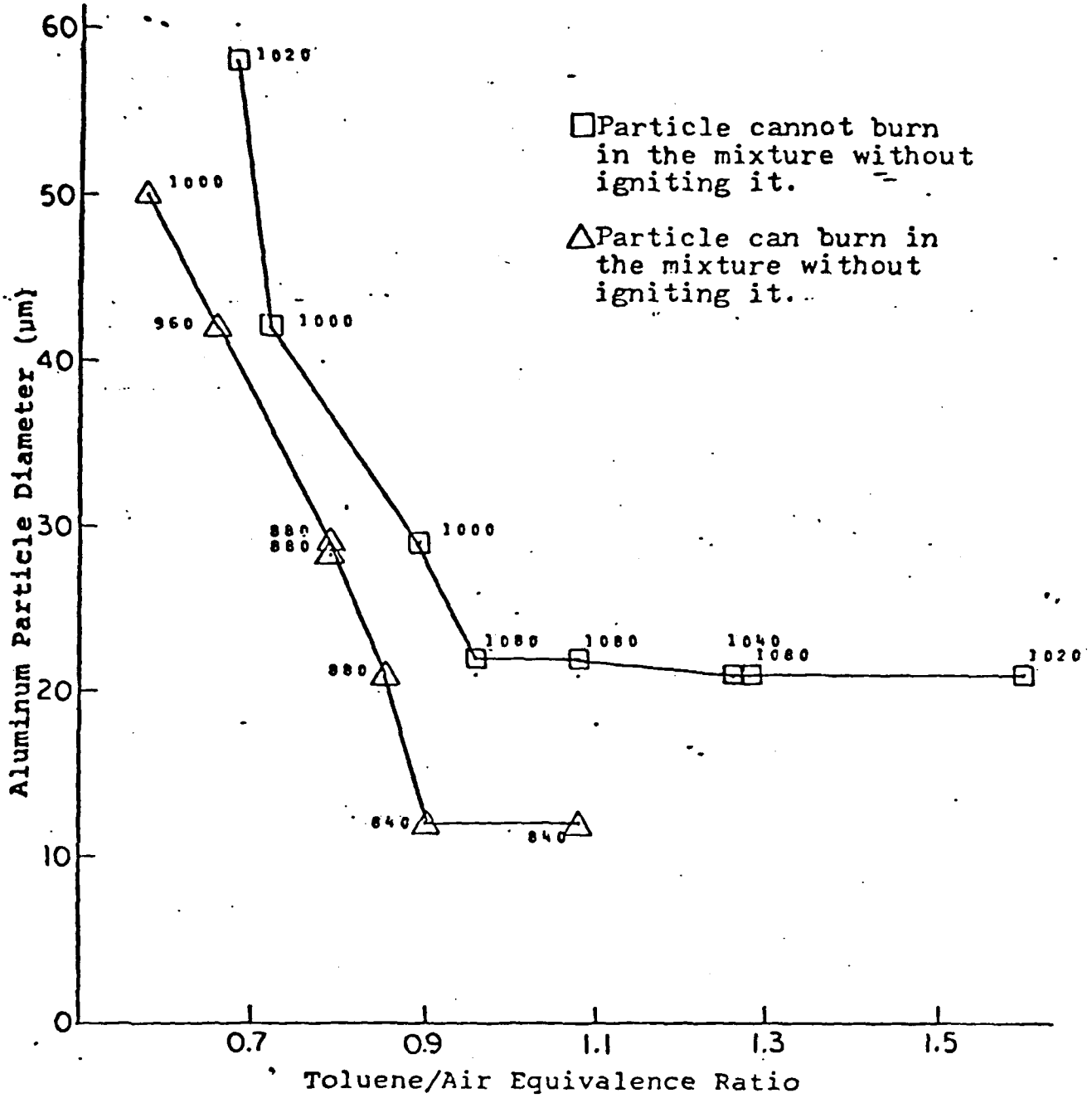

Figure 2: Critical Aluminum Particle Diameter vs. Toluene Equivalence Ratio

(inert or burning) metal particles has been completed. In particular, the minimum or critical particle size was determined as a function of the particle temperature, ambient gas temperature, and mixture ratio; propane gaseous fuel and air mixtures were considered. Both global (one-step) and semi-global (four-steps) chemical kinetics were examined. An unsteady spherically symmetric field around a hot particle was considered. The expansion of the gas due to heating was taken into account in the modelling. Both inert and burning particles were considered.

Two theoretical approaches were employed:

i. a finite-difference calculation, and

ii. asymptotic calculations were made.

One asymptotic analysis was made for the case where the particle temperature is comparable or higher than the gas adiabatic flame temperature. Another asymptote is analyzed when the adiabatic flame temperature is higher than the particle temperature. It was necessary to carry the low particle temperature asymptotic analysis to second order in the reciprocal of the nondimensional activation energy; otherwise good agreement is not obtained between numerical integration and the asymptotic theory.

The major conclusions of the theoretical development are represented in Figures 3 and 4. In the first figure, critical particle temperature is plotted versus critical particle size. These may be regarded as the minimum values of temperature and diameter to obtain ignition of the surround gas; that is, ignition is assumed above the curve. The basic curve is the result of a finite-difference calculation and may be regarded as an exact solution. (The details are provided in the paper by Su, Homan and Sirignano [3], in the paper by Su and Sirignano [4], and in the Ph.D. thesis of Y.P. Su.) It is seen that small particles must have high temperatures in order to serve as an adequate ignition source. Similarly, less hot particles must be larger to ignite a given mixture. The two asymptotic results agree well with the exact solution in their respective ranges of validity.

Figure 4 shows critical particle size as a function of equivalence ratio. A four-step propane oxidation mechanism was employed. The minimum critical size is slightly on the fuel rich side. The two figures indicate that chemical rates and transport rates are key in determining probability of ignition. Higher particle temperatures and near-stoichiometric mixtures result in faster chemical rates, thereby enhancing ignition. Smaller particles result in faster transport of heat and radicals away from the high temperature region thereby inhibiting ignition. These theoretical results are consistent with experimental results also reported herein. Precise comparison between theory and experiment will be made in the near future.

In the present study, one-dimensional transient calculations are conducted to examine the spray ignition process. A quiescent fuel-air mist in a one-dimensional tube is considered. One end of the tube is taken to be a hot isothermal surface, which acts as the ignition source. The other end can be either open or enclosed by an adiabatic surface. An Eulerian approach is used to solve the gas-phase equations,

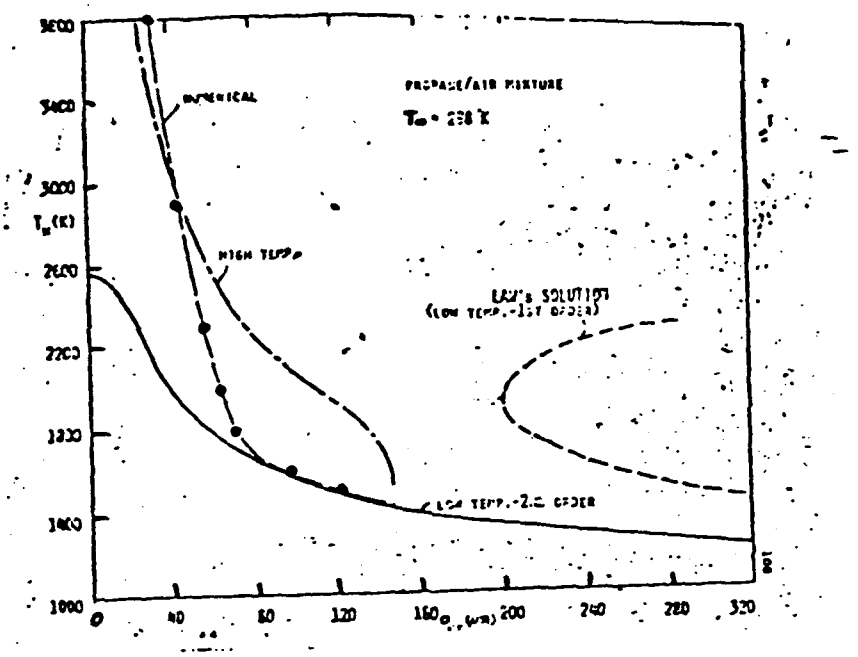

Figure 3:

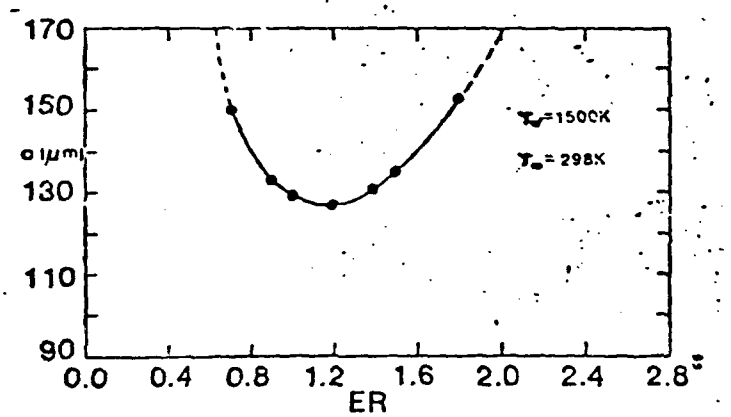

Figure 4:

whereas the liquid-phase equations are solved by a Lagrangian approach. Unsteady numerical computations are continued until the ignition is detected in the mixture. The occurrence of ignition is defined by the condition of zero heat flux at the hot surface. This marks the initiation of a propagating flame into the mixture. The physical model and the appropriate two-phase equations are given in the next section. Results are presented later, where effects of various parameters are also discussed. Parameters influencing the spray ignition process can be grouped into (a) the gas-phase parameters which include convective motion, turbulence, chemical kinetics and thickness of the thermal layer near the ignition source, (b) the liquid-phase parameters

which include fuel type, vaporization characteristics and spray characteristics such as droplet size distribution droplet spacings and locations, and (c) the ignition source parameters which may include its geometry, temperature and radiation characteristics. The ignition process is also affected by other considerations. For example, it is important to know (i) the nature of interaction between the droplets and the ignition source (ii) the nature of droplet-droplet interaction (iii) whether the droplets get ignited, i.e., envelope flames appear around individual droplets and (iv) whether the ignition source is inert or reacting. Effects of several of these parameters have been examined in the present study.

THE PHYSICAL MODEL AND THE GOVERNING EQUATIONS

The physical model is shown schematically in Fig. 5. It is used to study the ignition of fuel-air sprays in contact with a planar hot wall. Single-component fuel has been considered. The spray is characterized by monodisperse droplets. It is further assumed that the initial droplet locations can be represented in a deterministic sense. Implications of this assumption are discussed in a later section. The appropriate two-phase equations along with the gas-phase source terms are given as follows:

Gas-Phase Equations

$$\frac{\partial \rho}{\partial t} + \frac{\partial}{\partial x}(\rho V) = S_\rho \tag{1}$$

$$\frac{\partial Y}{\partial t} + V\frac{\partial Y}{\partial x} - \frac{1}{\rho}\frac{\partial}{\partial x}\left(\rho D \frac{\partial Y}{\partial x}\right) = S_Y \tag{2}$$

$$Y = Y_f,\ Y_O,\ \phi \tag{3}$$

$$\phi = T\, p^{\frac{1-r}{r}} \tag{4}$$

$$\rho = \frac{p^{1/r}}{\psi} \tag{5}$$

LIQUID-PHASE EQUATIONS

$$\frac{dx_k}{dt} = V_k \tag{6}$$

$$\frac{d\,V_k}{dt} = \frac{3}{16}\left\{\rho_r\, L_r^{\,2}\right\} C_D \frac{\mu}{r_k^{\,2}} Re_k\,(V-V_k) \tag{7}$$

$$\frac{d\,r_k^{\,2}}{dt} = -2\left\{\rho_r\, L_r^{\,2}\right\} \frac{\rho\, D}{\rho_k}\, m_k \tag{8}$$

where

$$Re_k = \frac{1}{L_r}\,\frac{2\, r_k \rho\, |V-V_k|}{\mu} \tag{9}$$

GAS-PHASE SOURCE TERMS

$$S_\rho = \frac{1}{L_r}\,\frac{1}{\Delta x}\sum_k m_k\, n_k \tag{10}$$

$$S_{Y_f} = \frac{-w\, M_f}{\rho} + \frac{S_\rho}{\rho}\,(1 - Y_f) \tag{11}$$

$$S_{Y_o} = \frac{-w\, M_o}{\rho}\,\psi - \frac{S_\rho}{\rho}\, Y_o \tag{12}$$

$$S_\phi = \frac{1}{p^{r-1/r}\rho\, C_p}\left\{w\, Q - \sum_k S_\rho \left(H + C_p(T-T_k)\right)\right\} \tag{13}$$

where

$$m_k = 4\pi\, \rho\, D\, r_k\, \bar{m}_k \tag{14}$$

$$\bar{m}_k = Re_f\, \ell n\, (1+B_k) \tag{15}$$

$$Re_f = (1 + 0.3\, Re_k^{*.5}) \tag{16}$$

$$w = C_f \exp(-T_a/T) \left(\frac{Y_f\, \rho}{M_f}\right)^a \left(\frac{Y_o\, \rho}{M_o}\right)^b \tag{17}$$

$$B_k = \frac{C_p(T - T_k) + S_f\, \nu\, Y_o\, Q}{H} \tag{18}$$

$$H = \frac{(1-Y_{fs})[C_p(T-T_k) + S_f\, \nu\, Y_o\, Q]}{S_f\, \nu\, Y_o + Y_{fs} - Y_f\,(1-S_f)} \tag{19}$$

S_f = 1 for burning droplet

= 0 for vaporizing droplet (20)

$$Y_{fs}^{-1} = 1 + \frac{M_a}{M_f}\left(x_{fs}^{-1} - 1\right) \tag{21}$$

(22)

$$x_{fs} = \frac{p'_n}{p'} \exp\left[\frac{L' M_f'}{R'} \left(\frac{1}{T_{bn}'} - \frac{1}{T_k'}\right)\right]$$

The above equations are written in non-dimensional form. For non-dimensionalization, the length scale L_c' is the length of the computational domain and the time scale $t_c' = L_c'^2/D_c'$, where D_c' is the characteristic gas diffusivity. The velocity scale is obtained from these two scales. The gas-phase properties are non-dimensionalized by using the respective initial properties. For the liquid-phase equations, the droplet location, velocity, and temperature are respectively non-dimensionalized by the gas-phase length, velocity and temperature scales. The droplet radius is non-dimensionalized by the initial droplet radius. The above non-dimensionalization gives rise to two additional dimensionless groups L_r and ρ_r; L_r is the ratio of gas-phase length scale and initial drop radius, and ρ_r is the ratio of reference gas and liquid densities.

The important assumptions made in writing these equations are that the gas pressure is spatially uniform, radiative heat transfer is negligible, the species diffusion follows Fick's law with equal mass diffusivities. For each pair, the specific heats are constant, and the gas-phase Lewis and Schmidt numbers are unity. In addition, the product $\rho D (= \mu)$ is assumed constant.

INITIAL AND BOUNDARY CONDITIONS

The initial conditions correspond to a quiescent mist of air and fuel droplets. The initial properties for both the phases are specified to be uniform. Droplet spacing and the number of droplets with each characteristic are prescribed after the equivalence ratio and the droplet size have been prescribed. For the species mass fractions, zero gradient boundary conditions are specified at x=0 and x=L (see Fig. 5). For the gas temperature, at x=0 an isothermal condition is used, whereas at x=L an adiabatic condition is used. Note that x=L can be an open or closed end.

RESULTS

Results for the ignition of n-octane/air spray are shown in Figs. 6-8 and Tables 2-10. The characteristics of the transient ignition process are displayed in Figs. 6-8. The ignition source supplies heat to the environment. As the environment temperature increases, the amount of heat supplied to the droplet increases and

vaporization is initiated. The resulting fuel vapor mixes with the oxidizer and the chemical reaction, which is weak initially, is started. Typical gas-phase and liquid-phase properties during this phase (at time = 10 msec) are shown in the figures. As the environment temperatures and the fuel vapor concentrations increase, chemical reactions intensify. Finally an ignition or temperature 'runaway' state is reached such that the combustion process becomes self-supporting, i.e. without any heat transfer from the ignition source. This ignition state is defined by the zero heat flux condition at the ignition source. The profiles of fuel vapor mass fraction and gas temperature at the time of ignition are shown in Figs. 6-7, respectively. The liquid-phase properties, i.e., the droplet location, size and temperature are given in Fig. 8. The droplet vaporization and the gas heating cause an expansion and movement of the gas so that the droplets are dragged away from the wall, as indicated in Fig. 8. These figures also indicate that the droplets nearest to the wall take the most active part in the ignition process.

Results of a parametric study are summarized in Tables 2-10. Values of various parameters used in the test case are shown in Table 1. n-Octane fuel droplets have been used for these calculations. For the results shown in Tables 2-10, the possibility of droplet ignition, i.e., of having envelope flame around individual droplets is included. A droplet ignition criterion as suggested by Law [11] is employed for this purpose. Implications of including droplet ignition are discussed later. The effect of hot wall temperature on the ignition delay time and ignition energy are portrayed in Table 2. Ignition delay time is defined as the time to reach the condition of zero heat flux at the hot wall, whereas the ignition energy is defined as the total heat per unit area conducted from the wall prior to the point of ignition. An increase in wall temperature leads to faster heating and vaporization, which leads to shorter ignition delays and reduced ignition energies.

Table 3 shows that the initial gas temperature has a modest effect on the ignition delay and the ignition energy. An increase in the initial gas temperature leads to faster vaporization and thus shorter ignition delay. As indicated in Table 4, the initial fuel vapor mass fraction has a small effect on the ignition delays and the ignition energies. Thus the initial fuel vapor mass fraction is not a very important parameter if the initial gaseous mixture is well on the lean side of the flammability limit. Most of the fuel vapor required for ignition must come from the droplets.

As shown in Table 5, the initial droplet size has strong effect on the ignition delays and ignition energies. Note that to keep the overall mixture ratio fixed as

initial droplet radius decreases, the number of droplets with each characteristic increases inversely as the square of the droplet radius and the droplet spacing decreases linearly with droplet radius. With a decrease in droplet size, ignition delay and ignition energy decrease until a minimum is reached. Further decrease in droplet size causes an increase in ignition time and ignition energy. This behavior is believed to be for two reasons. First, there is no envelope flame or individual droplet ignition for very small droplets. For example, with an initial drop radius of 13.12 microns, there is no envelope flame, whereas for drop radius of 26.25, 52.5 and 105 microns, the droplet nearest to the hot wall are individually burning. Since the vaporization rate for non-burning droplets is small, spray ignition takes longer time. The second reason for the above behavior is that as the droplet size is reduced, the fuel vapor distribution near the ignition source changes significantly, which in turn influences the ignition delay time and the ignition energy. As shown in Fig. 9, for droplet radius of 105, 52.5 and 26.25 microns, the fuel vapor mass fraction has a very steep front near the ignition source. Of course, the peak value of Y_f increases as the droplet size is reduced. For the droplet radius of 13.12 microns, the fuel vapor distribution is much more uniform and there is a large drop in the peak value of Y_f which increases the ignition delay time.

The difference between the burning-droplet case and non-burning-droplet case are further elucidated by comparing Tables 5 and 6 and Figs. 9 and 10. Note that in the burning-droplet case, a droplet ignition criterion is used to determine the possibility of an envelope flames around individual droplets. Results indicate that for drop sizes of 105.0, 52.5 and 26.25 microns, the droplets closest to the hot wall has envelope flame. For drop size of 13.12, there are no envelope flames. In the non-burning droplet case, individual droplets are not allowed to burn; they only vaporize. Figures 9 and 10 indicate that the fuel vapor distribution near the ignition source is markedly different for the burning-droplet and the non-burning-droplet cases, respectively. As a result, the droplet ignition has a strong influence on the spray ignition delay time and the ignition energy. As shown in Tables 5 and 6, especially for large droplets, the values of ignition delay time and ignition energy can vary significantly depending on whether the droplet ignition is considered or not.

The purpose of Table 7 is to demonstrate that the exact location of the droplet nearest to the ignition source can strongly influence the ignition delay time and the ignition energy. Part (a) of this table gives the effect of drop size when the nearest droplet is placed at .05 cm from the wall. Comparison of these values with those in

Table 5 shows that changing the location of the nearest droplet can produce large quantitative changes in the ignition delay time and the ignition energy. This is further substantiated in Table 7, part (b). The reason for this behavior is due to the fact that the average distance between droplets is of the same order as the gas thermal layer thickness at the hot wall that is developed during the ignition process (see Fig. 7). Since in practice the exact location of the droplet is not known, a statistical phenomenon is indicated. Thus, there is a need to study the ignition of fuel sprays by employing a probabilistic approach.

In order to examine the effects of fuel type, it seems appropriate to isolate the chemical kinetics effects and the vaporization effects. The influence of chemical kinetics is studied by varying the activation energy and the pre-exponential factor. The results are shown in Tables 8 and 9. An increase in activation energy results in an increase in the ignition delay time and the ignition energy. At higher values of the activation energies, the effect is much stronger since the ignition process becomes chemically controlled. Similar effects are observed by varying the pre-exponential factor. A decrease in this factor increases the ignition delay and the ignition energy. The effect is stronger at relatively lower values of the pre-exponent factor as the ignition process becomes chemically-controlled. An interesting result is observed by comparing the effects of pre-exponential factor for the spray case and the premixed gaseous case. In the latter case, the pre-exponential factor has a relatively stronger effect on the ignition delay and the ignition energy. This is due to the droplet vaporization process in the spray case, where the ignition process becomes vaporization-controlled at large values of pre-exponential factor. As seen in Table 9, the ignition delays and the ignition energies are higher for the spray case. At low values of pre-exponential factor, the ignition process becomes kinetically-controlled for both the cases. However, for the spray case, the mixture becomes locally fuel rich due to the sufficiently large time available for vaporization. This reduces the ignition delay and the ignition energy for this case as compared to the premixed case. Note that for one-step reaction scheme with unity exponents for fuel and oxidizer concentrations, the optimum equivalence ratio for the minimum ignition energy in the premixed case is about 9. This is shown in Table 10, which gives the effect of equivalence ratio for the spray and the premixed cases. It is interesting to note that the optimum equivalence ratios are so different for the two cases. The difference is due to the fact that for the spray case, the initial droplet distribution causes a stratification in the fuel vapor distribution. For example, even for the case when equivalence ratio is unity, a fuel-rich zone develops near the ignition source. It

is also noteworthy that in the spray case the optimum equivalence ratio for the minimum ignition time is different than that for the minimum energy.

The second effect, which is perhaps more significant, of changing the fuel type is due to its vaporization characteristics, i.e., the volatility. Table 11 gives the variation of the ignition time and the ignition energy with droplet radius for three different fuels, namely hexane, decane and hexadecane. The properties for these three fuels are given in Table 2. Note that the corresponding values for octane are given in Table 5. As expected, the fuel volatility has a strong influence on spray ignition. Moreover, the effect of fuel type is much more pronounced when the initial droplet size is large.

REFERENCES

1. Stanley, Thomas J., *Ignition of Combustible Mixtures by Burning Metal Particles*, Master's Thesis, Carnegie-Mellon University, 1981.

2. Homan, H.S. and W.A. Sirignano, "Minimum Mass of Burning Aluminum Particles Required for Ignition of Methane/Air and Propane/Air Mixtures", *Eighteenth Symposium (International) on Combustion*, the Combustion Institute, Pittsburgh, PA, p. 1709, 1981.

3. Su, Y.P., H.S. Homan and W.A. Sirignano, "Numerical Predictions of Conditions for Ignition of a Combustible Gas by a Hot, Inert Particle", *Combustion and Science Technology*, December 1978.

4. Su, Y.P. and W.A. Sirignano, "Ignition of a Combustible Mixture by an Inert Hot Particle", *Eighteenth Symposium (International) on Combustion*, the Combustion Institute, Pittsburgh, PA, 1981.

5. Miyasaka, K. and Mizutani, Y., "Ignition of Sprays by an Incident Shock," *Combustion and Flame*, Vol. 25, pp. 177-186 1975.

6. Miyasaka, K. and Mizutani, Y., "Ignition Delays of Spray Columns Behind a Reflected Shock," *Sixteenth Symposium (International) on Combustion*, The Combustion Institute, Pittsburgh, PA, pp. 639-645, 1976.

7. Ballal, D.R. and Lefebvre, A.H., "Ignition and Flame Quenching of Quiescent Fuel Mist," *Proc. Roy. Soc.* A 364, pp. 277-294, 1978.

8. Ballal, D.R. and Lefebvre, A.H., "A General Model of Spark Ignition for Gaseous and Liquid Fuel-Air Mixtures," *Eighteenth Symposium (International) on Combustion*, The Combustion Institute, pp. 1737-1746, 1981.

9. Peters, J.E. and Mellor, A.M., "An Ignition Model for Quiescent Fuel Sprays," *Combustion and Flame* Vol. 38, pp. 65-74, 1980.

10. Chan, K.K. and Polymeropoulos, C.E., "An Experimental Investigation of the

Minimum Ignition Energy of Monodisperse Sprays," Eastern Section/ Combustion Institute, Fall Technical Meeting, October 27-29, 1981, Pittsburgh, PA.

11. Law, C.K., "Asymptotic Theory for Ignition and Extinction in Droplet Burning," *Combustion and Flame*, Vol. 24, pp. 89-98 (1975).

Table 1: VALUES OF VARIOUS PARAMETERS USED IN SPRAY IGNITION STUDY (TEST CASE)

Parameter	Value
Fuel	n-octane
a	1
b	1
C'_{pc}	0.25 cal/gm/°K
C'_f	10^{14} cm^3 mole^{-1} sec^{-1}
C'_{pl}	0.526 cal/gm/°K
d'_s	0.2 cm
L'	86.25 cal/gm
L'_c	2.0 cm
M'_a	28.9 gm/mole
M'_f	114 gm/mole
M'_o	32 gm/mole
n'_k	20 1/cm^2
P'_c	1 atm
Q'	10700 • M'_f cal/mole
R'	1.98717 cal/mole
r'_{ko}	52.5 microns
T'_a	40000.0/R' °K
T_w	1500 °K
T'_{bn}	398.8 °K
T'_k	300 °K
T'_c	400 °K
Y_{fi}	0.01

$\Delta x'$	.02 cm
$\Delta t'$	10^{-5} sec
γ	1.38
$\mu' = \rho_c' D_c'$	1.8446×10^{-4} gm/cm/sec
ρ_ℓ'	0.707 gm/cm^3
Ψ	=12.5

Table 2: EFFECT OF HOT WALL TEMPERATURE

T_{wall} * <K>	Ignition Time (m sec)	Ignition Energy ($mcal/cm^2$)
2000	5.31	3.743
1800	8.15	5.328
1600	13.31	7.283
1500	18.17	8.658
1400	27.69	10.643
1300	54.71	14.127
1200	No ignition up to 160 msec.	

Table 3: EFFECT OF COLD GAS TEMPERATURE

T_{gas} (°K)	Ignition Time (m sec)	Ignition Energy (mcal/cm^2)
400	14.25	7.362
350	15.91	8.011
320	17.46	8.472
310	18.17	8.658

Table 4: EFFECT OF INITIAL FUEL VAPOR MASS FRACTION

$Y_{F\ vapor}$	Ignition Time (m sec)	Ignition Energy (mcal/cm^2)
0.01	18.17	8.658
0.005	18.67	8.912
0.002	18.97	9.067
0.001	19.07	9.118

Table 5: EFFECT OF DROPLET SIZE (Burning-Droplet Case)

(First characteristic at 0.02 cm from the wall)

Droplet Radius (μm)	Ignition Time (m sec)	Ignition Energy (mcal/cm^2)
105	14.79	7.89
52.5	8.98	5.98
26.25	7.25	5.25
13.125	10.4	5.56
Premixed	11.54	5.54

Table 6: EFFECT OF DROPLET SIZE (NON-BURNING DROPLET CASE)

(First characteristic at 0.02 cm from the wall)

Droplet radius (μm)	Ignition Time (m sec)	Ignition Energy (mcal/cm^2)
105.0	23.45	9.38
52.5	12.10	6.72
26.2	8.51	5.50
13.1	10.40	5.56

Table 7: (a) EFFECT OF DROPLET SIZE

(First characteristic at 0.05 cm from the wall)

Droplet Radius (μm)	Ignition Time (m sec)	Ignition Energy (mcal/cm^2)
105	20.69	9.1
52.5	14.25	7.36
26.25	13.92	6.82
13.125	17.25	7.1

(b) EFFECT OF DISTANCE BETWEEN THE HOT WALL AND THE NEAREST CHARACTERISTIC

Distance(cm)	Ignition Time (msec)	Ignition Energy (mcal/cm^2)
.01	8.43	5.50
.02	8.98	5.98
.03	10.25	6.31
.04	12.09	6.81
.05	14.44	7.43
.05	14.44	7.43
.06	17.62	8.17

Table 8: EFFECT OF ACTIVATION ENERGY

Activation Energy (Kcal/mole)	Ignition Time (msec)	Ignition Energy ($mcal/cm^2$)
35	4.35	3.78
38	6.49	4.90
40	8.90	5.95
42	12.92	7.39
44	19.85	9.39
46	30.84	11.82

Table 9: (a) EFFECT OF PRE-EXPONENTIAL FACTOR (SPRAY CASE)

Pre-Exponential Factorx10^{-14} ($cm^3 mole^{-1} sec^{-1}$)	Ignition Time (msec)	Ignition Energy– ($mcal/cm^{-2}$)
10	4.05	3.65
8	4.30	3.80
5	4.93	4.15
2	6.69	5.02
1	8.90	5.95
.5	12.60	7.24
.2	21.94	9.76
.1	41.00	12.31

(b) EFFECT OF PRE-EXPONENT FACTOR (PRE-MIXED CASE)

Pre-Exponential Factorx10^{-14} ($cm^3 mole^{-1} sec^{1}$)	Ignition Time (msec)	Ignition Energy ($mcal/cm^2$
10	3.07	2.67
8	3.36	2.82
5	4.16	3.19
2	6.98	4.26
1	11.54	5.54
.5	20.28	7.42
.2	43.95	11.14
.1	79.14	15.24

Table 10: EFFECT OF EQUIVALENCE RATIO

(a) Spray Case

ϕ	Ignition Time (msec)	Ignition Energy ($mcal/cm^2$)
0.5	10.62	6.15
0.8	9.34	5.97
1.0	8.98	5.98
2.0	8.95	6.621
3.0	10.18	7.79
4.0	12.83	9.51
5.0	20.09	12.30
6.0	31.79	16.08

(b) Pre-Mixed Case

ϕ	Ignition Time (msec)	Ignition Energy ($mcal/cm^2$)
.5	26.73	8.04
.8	14.43	6.15
1.0	11.54	5.54
2.0	6.89	4.27
3.0	5.64	3.83
4.0	5.09	3.61
5.0	4.79	3.49
6.0	4.63	3.41
7.0	4.54	3.37
8.0	4.50	3.346
9.0	4.49	3.335
10.0	4.5	3.335
11.0	4.54	3.343
12.0	4.59	3.357

Table 11: EFFECT OF DROPLET RADIUS FOR DIFFERENT FUELS

(a) Fuel: Hexane

Radius (μm)	Ignition Time (msec)	Ignition Energy (mcal/cm^2)
105.00	10.60	6.23
52.50	8.04	5.43
26.25	7.02	5.03
13.12	10.58	5.586
	Fuel: Decane	
105.00	22.64	10.14
52.5	10.64	6.755
26.25	7.41	5.377
13.12	11.2	5.656
	Fuel: Hexadecane	
105.00	48.88	15.30
52.50	17.29	9.171
26.25	8.53	6.012
13.12	9.98	5.474

Table 12: FUEL PROPERTIES

	HEXANE	OCTANE	DECANE	HEXADECANE
W_f'(gm/mole)	86.18	114.00	142.30	226.45
ν'	9.5	12.5	15.5	24.5
ρ_ℓ'(gm/cm^3)	.659	.707	.73	.773
L'(cal/gm)	88.5	86.5	76.7	68.03
Cp'_ℓ(cal/gm/°K)	.526	.526	.526	.526
$k_\ell' \times 10^6$ (cal/cm/sec/°K)	226.5	226.5	226.5	226.5
T'_{bn}(°K)	341.9	398.8	447.3	560.

NOMENCLATURE

a,b	exponents of fuel and oxidizer concentrations, respectively.
$Cp'=Cp\ Cp_c'$	specific heat at constant pressure, cal/gm/°K
$Cp_k'=Cp_k\ Cp_c'$	liquid specific heat
$C_f'=C_f(\rho_c'/M_c')^{1-a-b}$	pre-exponent factor, $(\text{mole cm}^3)^{1-a-b}\text{sec}^{-1}$
d_s'	droplet spacing, cm
$D'=D\ D_c'$	gas diffusivity, cm^2/sec
E_a'	activation energy, cal/mole
$H'=H\ C_{pc}'T_c'$	heat given to the droplet per unit mass, cal/gm
L_c'	characteristic length scale, also the length of the computational domain
$L'=L\ Cp_c'\ T_c'$	heat of vaporization, cal/gm
L_r	L_c'/r_{ko}'
$M_f'=M_f M_c'$	molecular weight of fuel, gm/mole
$M_o'=M_o M_c'$	molecular weight of oxidizer, gm/mole
$m_k'=m_k \rho_c' D_c' r_{ko}'$	vaporization rate of a droplet, gm/sec
$n_k'=n_k/L_c'^2$	number of droplets with each characteristic, $1/\text{cm}^2$
$p'=p\ p_c'$	pressure, atm
p_n'	normal pressure, 1 atm
$Q'=Q\ Cp_c'\ T_c'\ M_c'$	heating value of fuel, cal/mole
$r_k'=r_k\ r_{ko}'$	droplet radius, cm
R'	gas constant, 1.98717 cal/mole/°K
$t'=t\ t_c'$	time, sec
$t_c'=L_c'^2/D_c'$	characteristic time scale
$T_a'=T_a\ T_c'$	activation temperature, °K
T_{bn}'	boiling temperature at normal pressure

$T'=T\ T_c'$	gas temperature
$T_k'=T_k T_c'$	droplet surface temperature
$V'=V\ V_c'$	gas velocity, cm/sec
$V_k'=V_k\ V_c'$	droplet velocity
$X_k'=X_k\ L_c'$	droplet location, cm
X_{fs}	fuel vapor mole fraction at the droplet surface
$x'=x\ L_c$	spatial coordinate
Y	mass fraction
Y_{fs}	fuel vapor mass fraction at the droplet surface
Y_{fi}	initial fuel vapor mass fraction
$\Delta x'=\Delta x\ L_c'$	spatial grid size, cm
$\Delta t'=\Delta t\ t_c'$	temporal step size, cm
ϕ	transformed temperature (see Equation 4)
γ	ratio of specific heats
$\mu'=\mu\ \rho_c'D_c'$	viscosity, gm/cm/sec
ν	$M_f'/\psi M_o'$
$\rho'=\rho\ \rho_c'$	gas density, gm/cm^3
$\rho_r=\rho_c'/\rho_k'$	ratio of reference gas and liquid densities
ψ	molar stoichiometry ratio of oxidizer and fuel

LIST OF PROFESSIONAL PERSONNEL

Professor W.A. Sirignano

Professor E. Suuberg

Professor H.T. Sommer

Dr. S.K. Aggarwal

Mr. K.A. Thallner

DEGREES RECEIVED

K.A. Thallner, Master of Science degree

PUBLICATIONS RESULTING FROM RESEARCH

- H.S. Homan and W.A. Sirignano, "Minimum Mas of Burning Aluminum Particles for Ignition of Methane/Air and Propane/Air Mixtures," *Proc. 18th International Symposium on Combustion*, Combustion Institute, 1981.

- Y.P. Su, H.S. Homan, and W.A. Sirignano, "Numerical Predictions of Conditions for Ignition of a Combustible Gas by a Hot, Inert Particle," *Combustion Science and Technology*, December 1978.

- Y.P. Su and W.A. Sirignano, "Ignition of a Combustible Mixture by an Inert Hot Particle," *Proc. 18th International Symposium on Combustion*, Combustion Institute, 1981.

- T.J. Stanley, K. Thallner, J. Witt, A. Yee, W.A. Sirignano, and E.M. Suuberg, "The Ignition of Toleune/Air Mixtures by Burning Metal Particles," *Chemical and Physical Processes in Combustion*, Eastern Section/Combustion Institute, Pittsburgh, PA, October 1981.

- W.A. Sirignano, "Fuel Droplet Vaporization and Spray Combustion Theory," to appear in *Progress in Energy and Combustion Science*, 1983.

- Y.P. Su, "Ignition of Combustible Mixtures by Metal Particles," Ph.D. Dissertation, Princeton University, 1980.

- T.J. Stanley, "Ignition of Combustible Mixtures by Burning Metal Particles," Masters Thesis, Carnegie-Mellon University, 1981.

- K.A. Thallner, "The Ignition of Toleune/Air Mixtures by Burning Metal Particles," Masters Thesis, Carnegie-Mellon University, 1982.

OTHERS INTERESTED IN RESEARCH EFFORT

M. Hertzberg
U.S. Bureau of Mines

J. Mannheim
Aeropropulsion Laboratories
Wright-Patterson

L. Mahood
Falcon Research and Development

Professor A. Lefebvre
Purdue University

Professor S. Wojcicki
Warsaw Technical University

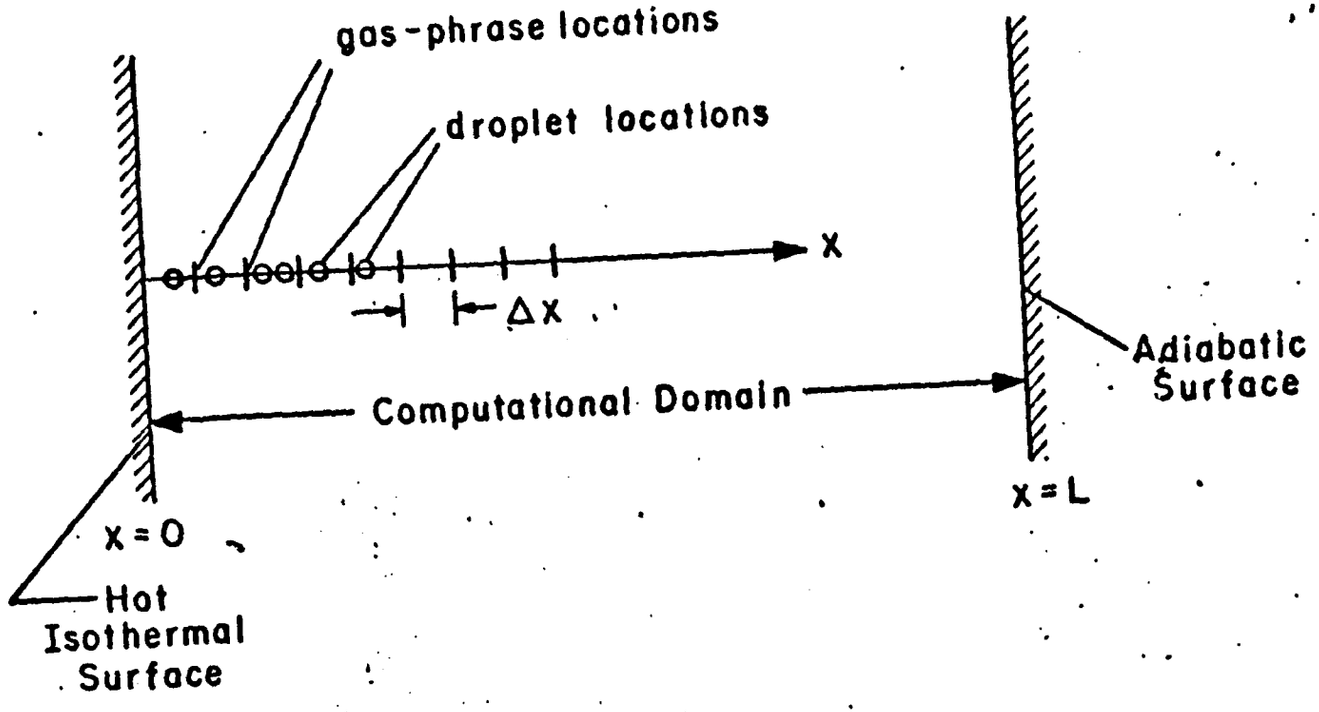

Fig. 5 Schematic of the Physical Model for Spray Ignition

Fig. 6

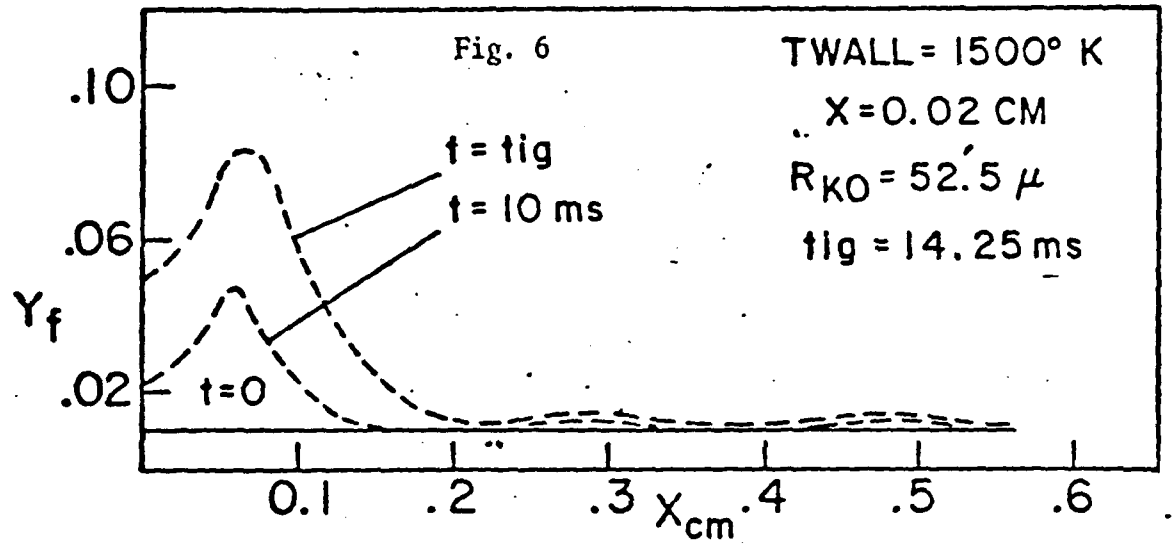

Fuel Vapor Mass Fraction Profiles Near the Hot Surface

Fig. 7

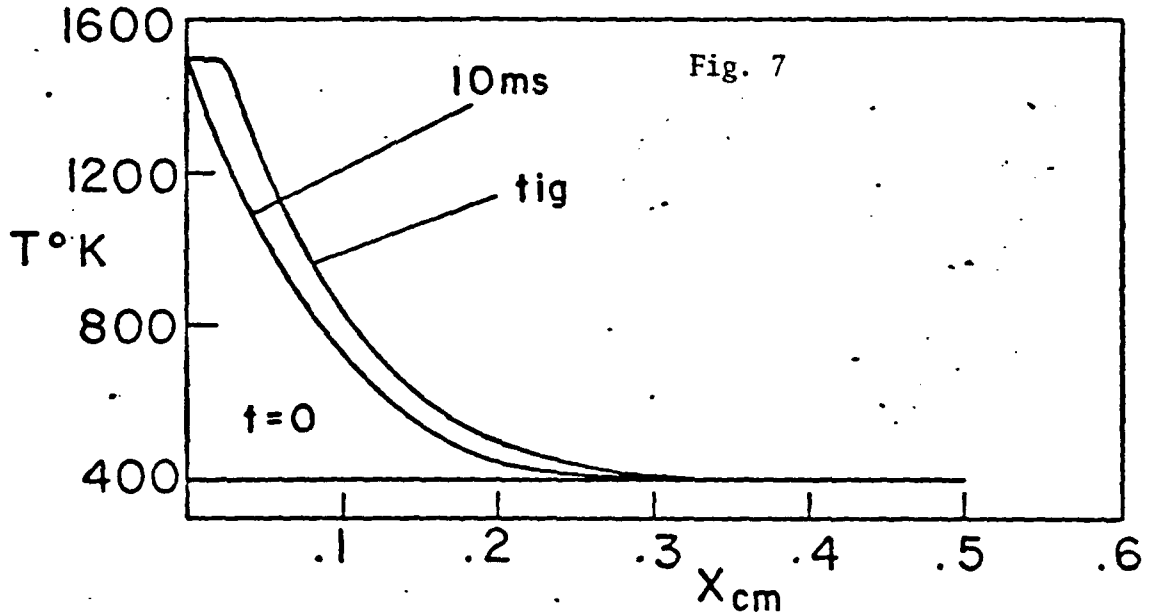

Gas Temperature Profiles Near the Most Hot Surface

Fig. 8

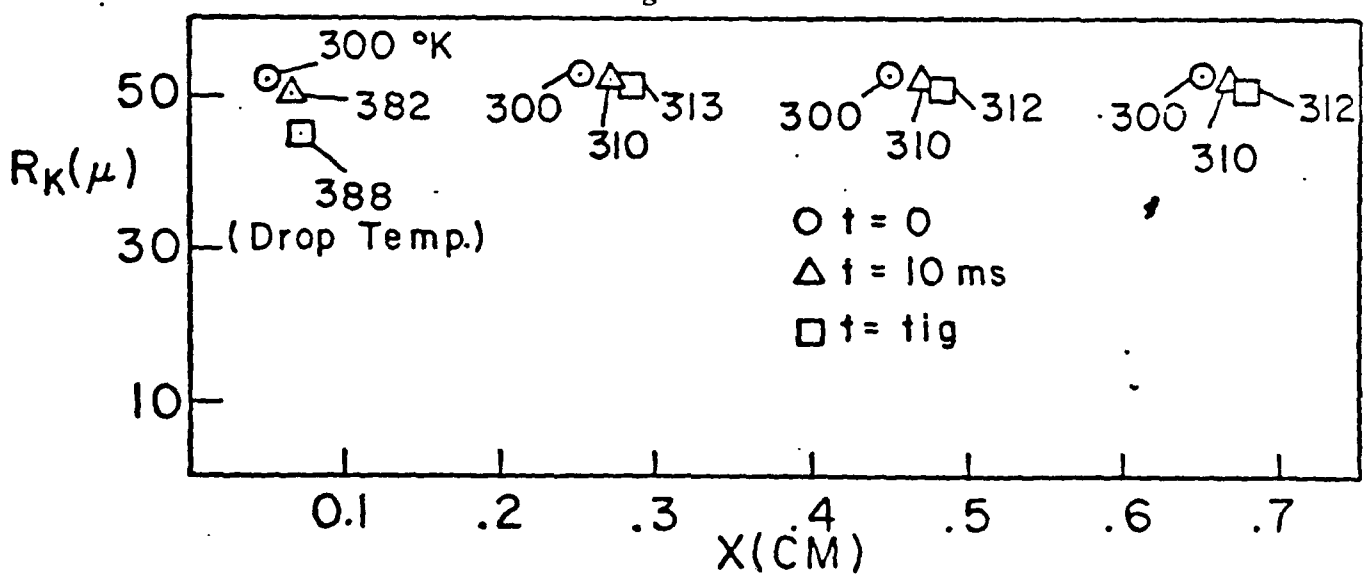

Variation of Droplet Properties With Time

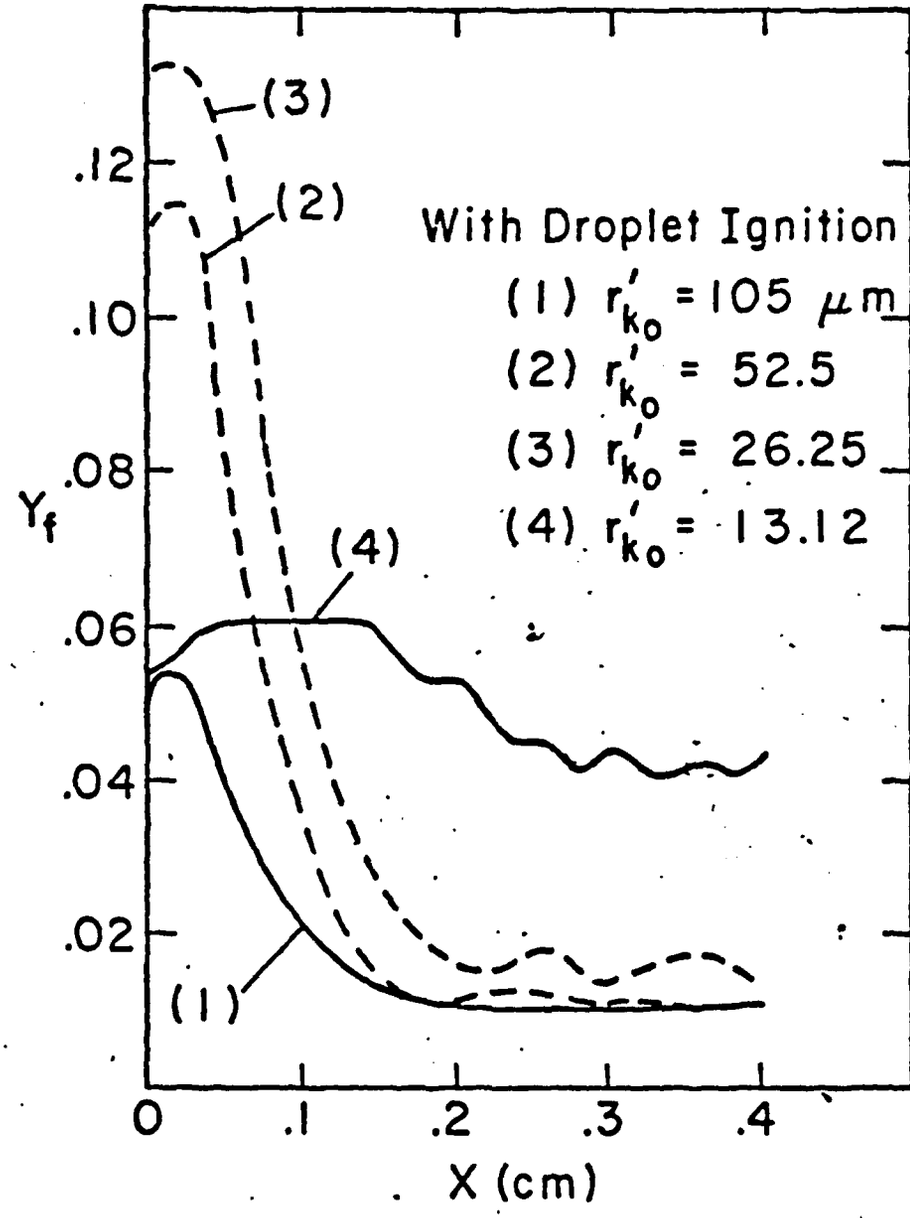

Fig. 9 Fuel Vapor Distribution Near the Hot Wall at the Time of Ignition for Different Drop Sizes

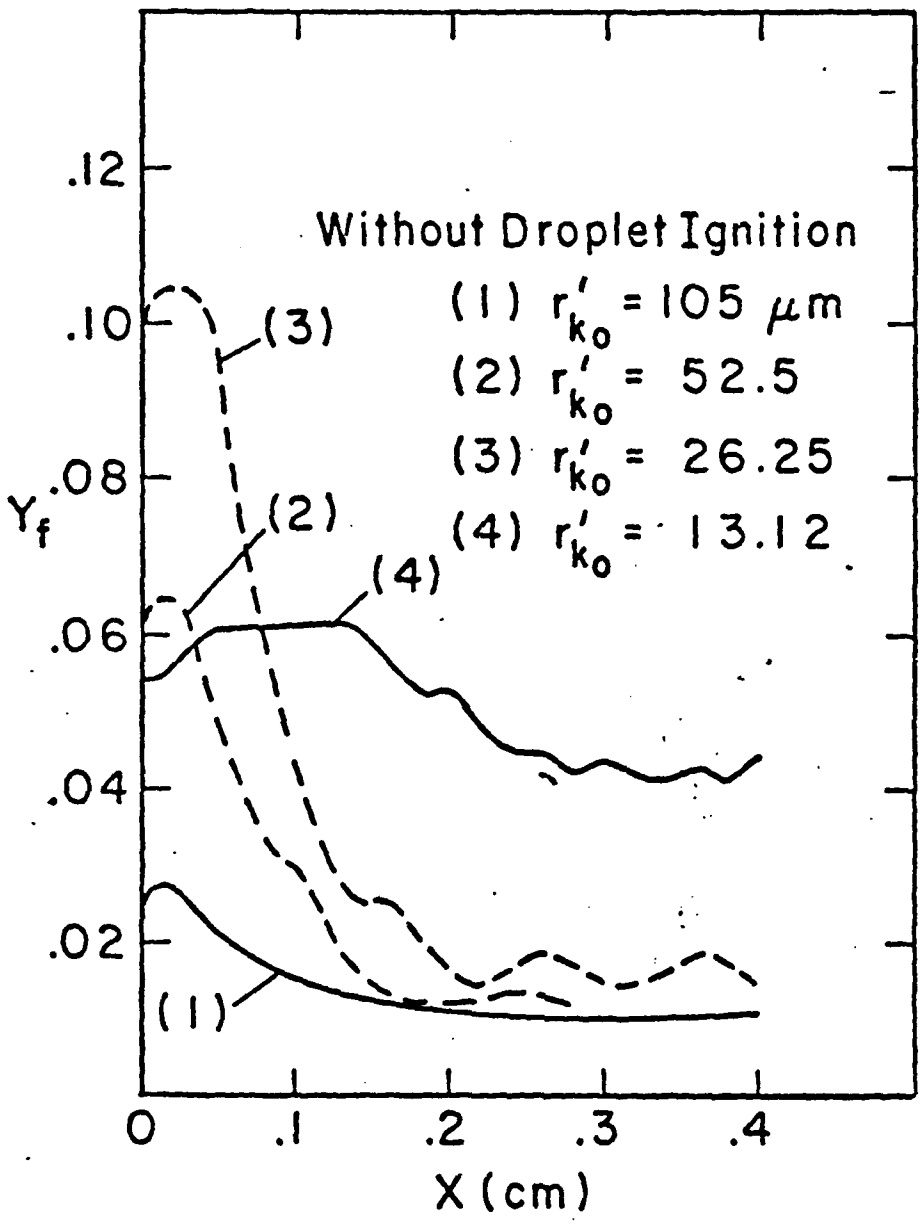

Fig. 10 Fuel Vapor Distribution Near the Hot Wall of the Time of Ignition for Different Drop Sizes